

Remodeling of integrated contractile tissues and its dependence on strain-rate amplitude
– Supplementary Information –

Madavi Oliver, Tímea Kováts, Srboj M. Mijailovich, James P. Butler, Jeffrey J. Fredberg, Guillaume Lenormand*

School of Public Health, Harvard University, Boston, MA, 02115, USA
*glenorma@hsph.harvard.edu

Table of content

Methods	1
Supplement 1: The elastic and loss moduli are measured from force-length loops.	3
Supplementary Figure 1: Force-length loops.	3
Supplement 2: The central roles of nonlinearity and strain amplitude.	4
Supplement 3: Analogy with inert fragile matter.	5
Supplementary Methods for cardiomyocyte experiments	6
Supplementary Figure 2	8
Supplementary Figure 3	9
Supplementary Figure 4	10
Supplementary References	11

Methods

Airway smooth muscle (ASM) strip preparation and experimental set-up: To perform the different protocols, we used two experimental set-ups. The Cambridge Technologies Lever Arm System, referred as system 1, is described in detail in Fredberg et al. [1] and the Scientific Instruments Muscle Research System, referred as system 2, is described in detail in Latourelle et al. [2]. A freshly isolated sheep trachea muscle strip (4.5×1.5×12 mm in system 1; 0.4×0.4×8 mm in system 2) is placed between a length transducer and a force transducer. Using a LabView code developed in our laboratory, the length signal is imposed and the resulting force signal is measured. Experiments are performed in KREBS solution at 37°C for system 1 and at room temperature for system 2. At the beginning of an experiment, the ASM strip is activated to obtain a maximal muscle contraction and is brought to a reference length, L_{ref} , using electric field stimulation in system 1 or 2×10^{-5} M acetylcholine (Ach) in system 2. After equilibrating at L_{ref} for 30 min, the muscle is subjected to sinusoidal length variations of amplitude ΔL , at frequency, f , about its reference length, L_{ref} : $L(t) = L_{ref} + \Delta L \sin(2\pi ft)$, and the resulting total force, F_T , is measured. When specified, acetylcholine is used for activation at 10^{-4} M and 2×10^{-5} M for system 1 and system 2 respectively.

Calculation of storage and loss moduli, E' and E'' : In activated airway smooth muscle, imposition of a sinusoidal change of length results in a force-length loop that can depart

dramatically from an elliptical shape, and thus reveals evidence of strong nonlinearity. (Supplementary information 1). Although linear analysis and Fourier decomposition become problematic in that case, effective storage and loss moduli can be defined nonetheless in terms of two unambiguous measures of the loop [1, 3, 4]: the amplitude of the force variation, ΔF , and the energy dissipated per cycle, Φ , the latter of which corresponds to the circumscribed area or hysteresis. For imposed frequency, f , and length change, ΔL , fluctuating about operating length about L_{ref} , $E' = (\Delta F/A)/(\Delta L/L_{\text{ref}})\cos \phi$, $E'' = (\Delta F/A)/(\Delta L/L_{\text{ref}})\sin \phi$, A is the cross sectional area, and the loss tangent $\eta = \tan \phi$, where $\phi = \sin^{-1}[\Phi/(\pi\Delta F\Delta L)]$. For linear systems, these relationships reduce to standard definitions, and are thus applicable to linear and nonlinear systems alike [1, 3, 4].

Computations of the perturbed acto-myosin bridge dynamics: To assess the quantitative contribution of bridge kinetics to the rheology of smooth muscle, numerical computations were performed using the latch regulation scheme of Hai and Murphy [5, 6] integrated with Huxley's sliding filament theory of muscle contraction [7]. The mathematical formulation of this model, numerical solution and parameter values used in the computations are described in Mijailovich et al. [8]. Computations strictly followed the protocol used on muscle strips where the strain-rate amplitude was held constant as the frequency of the oscillatory strain deformation was progressively increased. In the computations, the crossbridge strain amplitude, $\Delta\varepsilon_{XB_0}$ is assumed to be equal to 36% of the overall strain amplitude in muscle strip, $\Delta\varepsilon$, to account for the serial elastic component [8]. From closed stress-strain loops, we calculated the dynamic moduli, E' and E'' , for the range of the prescribed strain-rates.

Supplement 1: The elastic and loss moduli are measured from force-length loops.

Muscle rheology is innately nonlinear, and force-length loops have a characteristic “banana shape” (Supplementary Figure 1) [3]. In analyzing such loops, Fourier analysis is problematic. Nonetheless, for each such banana-shaped loop, one can define precisely and unambiguously the peak energy stored and the total frictional energy lost [3, 4]. Therefore, as summarized in Methods, one can define an effective storage (or stiffness) modulus, E' , and an effective loss modulus, E'' , which are readily quantified. These methods were developed by us long ago [4], and have come into standard use for assessment of cyclic forcing in nonlinear physiological systems.

Supplementary Figure 1:

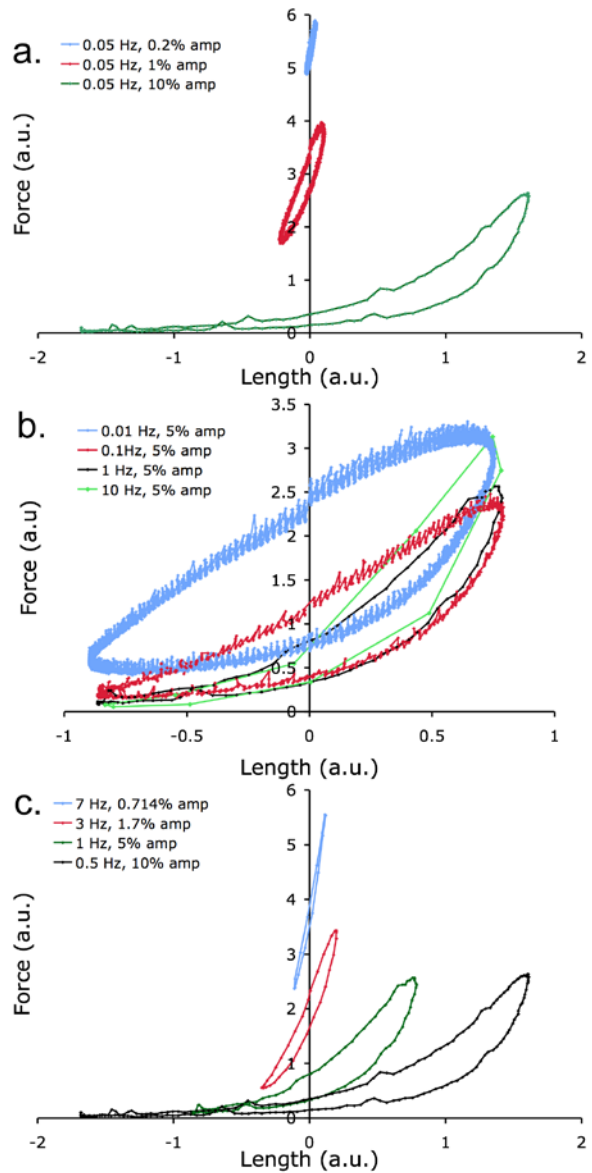
Force-length loops.

a. Fixed frequency (0.5 Hz) with increasing strain amplitude (0.2%, 1%, and 10% of L_{ref}).

b. Fixed strain amplitude (5%) with increasing frequency (0.01, 0.1, 1, and 10 Hz).

c. Fixed strain-rate amplitude (31.4 s^{-1}). As strain amplitude increases frequency decreases.

a.u. stands for arbitrary units.



Supplement 2: The central roles of nonlinearity and strain amplitude.

We consider a system with a relaxation time, τ , in which case $E' = \omega^2 k \tau^2 / (1 + \omega^2 \tau^2)$ and $E'' = \omega k \tau / (1 + \omega^2 \tau^2)$. Wyss et al. [9] proposed that structural relaxation and the corresponding relaxation time, τ , of a fragile system driven by imposition of an external fluctuation in strain at angular frequency ω , can be described by $1/\tau \approx 1/\tau_0 + \langle x \rangle \omega$, where τ_0 is the intrinsic relaxation time of the material or cell driven by spontaneous molecular rearrangements, and $\langle x \rangle$ is an index of the amplitude of imposed strain fluctuation, such as its amplitude or root mean square value. In the limit where $1/\tau_0 \ll \langle x \rangle \omega$, then $E' = k / (1 + \langle x \rangle^2)$ and $E'' = k \langle x \rangle / (1 + \langle x \rangle^2)$. The moduli are thus functions only of strain and are independent of frequency; this is compatible with data depicted in Fig. 2b.

Supplement 3: Analogy with inert fragile matter.

At fixed but small strain amplitude, rheology is scale-free: The stiffness of a cell in culture increases as a weak power law in frequency [10-15]. Such a frequency dependence cannot be characterized by an internal time scale or a time constant; therefore these responses are said to be scale-free [10-15]. Here we ask, is this scale-free behavior a peculiarity of the isolated cell in culture, or does it scale up to integrated airway smooth muscle tissue? To answer this question, we imposed length oscillations of small amplitude (0.5% of L_{ref}) and measured the elastic modulus, $E'(f)$, and the loss modulus, $E''(f)$, of the fully activated muscle. Over four frequency decades (from 10^{-2} to 10^2 Hz), $E'(f)$ approximates a weak power law, $E'(f) \sim f^{0.05}$ (Supplementary Figure 2a). The loss modulus, $E''(f)$, decreases slowly as the frequency increases, with a power law exponent close to -0.15 (Supplementary Figure 2a); this behavior has been observed in many glassy systems [9, 16-18], and do not violate the Kramer-Kroening relationship [19], which does not require the local slopes to be similar. As the frequency is increased, the loss tangent, η , decreases (Supplementary Figure 2a).

As strain-amplitude increases, the system fluidizes: At a fixed but arbitrary frequency in the middle of the experimental range (1 Hz), we increased the strain amplitude of the imposed length oscillation, γ_0 , progressively from 0.25% to 16% of L_{ref} while measuring $E'(f)$ and $E''(f)$ (Supplementary Figure 2b). As previously shown, for strain up to 1% of L_{ref} the ASM strip shows a limited linear range [3]. As the applied strain is increased further, however, progressive decreases of E' and E'' are observed, demonstrating a strong nonlinear behavior characterized by shear thinning with no evidence of strain hardening. At higher strain amplitudes, both E' and E'' decrease with strain as a power law with an exponent close to 1, ($\approx \gamma_0^{-1}$). As the strain amplitude increases, the loss tangent, η , increases from 0.1 to 0.3 (Supplementary Figure 2b) [3].

Recovery following a large transient stretch is slow and anomalous: We then studied recovery following one cycle of an oscillatory length change. After 1 hr of maximum isometric force contraction, we imposed one length oscillations about L_{ref} with amplitudes ranging from 0.25 to 16% of L_{ref} (at 1 Hz; Supplementary Figure 3), and tracked the evolution of E' and E'' using the lowest amplitude (0.25%). Following a length oscillation of 4% or less, E' remained almost unchanged (Supplementary Figure 3a). But with larger length oscillations, E' was promptly depressed in a dose dependent manner; upon stretch cessation E' slowly recovered (Supplementary Figure 3a). Therefore, a single brief stretch caused dramatic long-lasting effects. Following the transient stretch, the loss tangent, η , increases in a dose dependent manner, and then slowly recovers (Supplementary Figure 3b). An increase of η indicates a liquid-like behavior; therefore a single stretch fluidize the ASM trip, a behavior well described at the cellular level [20-23].

Cardiomyocyte, which cytoskeleton exhibits organized and striated structures, does not display scale-free rheology: Glassy dynamics is thought to be a consequence of structural disorder and metastability [18]. As a negative control, we show here that a cardiomyocyte, which cytoskeleton exhibits organized and striated structures, does not display scale-free rheology.

Cardiomyocytes are a specialized form of striated muscle where actin and myosin filaments are aligned in very orderly arrays to form a series of contractile units called sarcomeres. The sarcomeres are delimited by the so-called Z-line and are arranged into myofibrils. This organization was visualized using immunostaining of the Z-lines (Supplementary Figure 4a). Two successive Z-lines delimit a sarcomere, a succession of sarcomeres forms a myofibril spanning several tens of microns and over several living cells, as shown when the nuclei were visualized using DAPI staining (Supplementary Figure 4b). When the elastic, g' , and loss, g'' , moduli were measured over 4 decades in frequency, a clear departure from a power law behavior was observed (Supplementary Figure 4c). Therefore, cardiomyocyte dynamics cannot be considered scale-free. This dynamics is similar to that of striated muscles where the lump in the frequency dependence between 10 and 100 Hz is hypothesized to arise from rate constants in the actomyosin ATPase cycle [24].

Methods for cardiomyocyte experiments

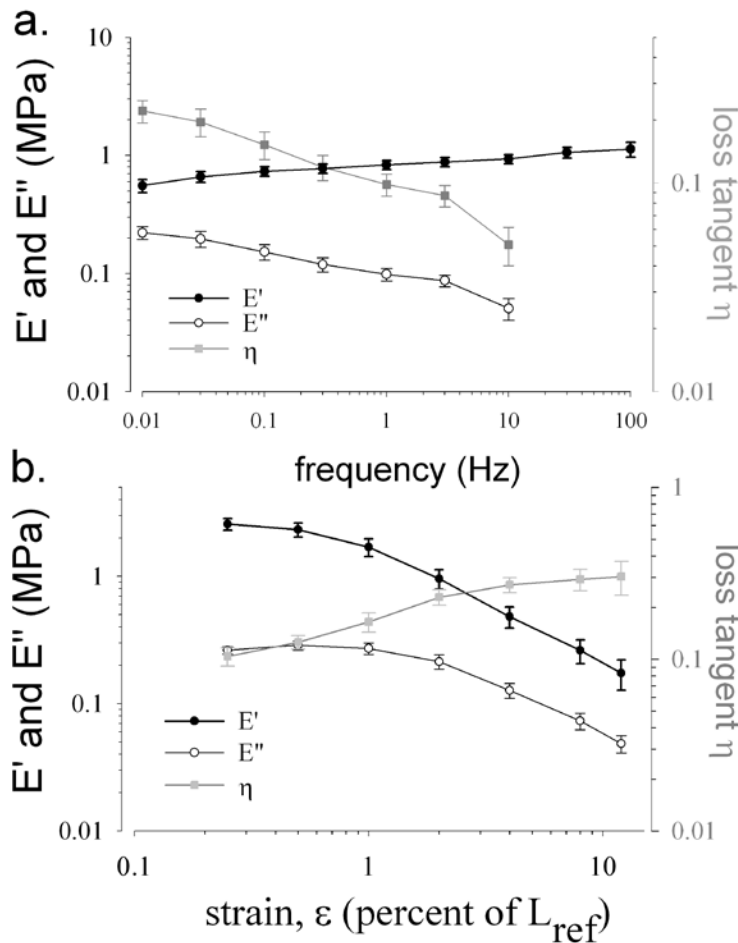
Cardiomyocyte preparation: Atrial and ventricle cardiomyocytes were obtained from isoflurane anesthetized 1 or 2 days old Sprague-Dawley rats. Atria and ventricles were dissociated under the microscope and processed separately. Following overnight trypsinization at 4°C, cells were released by subsequent repeated collagenase digestion at 37°C (Worthington). Cells were plated at high density (10^5 /well) on fibronectin and collagen coated 24-well plates and incubated overnight in a 4:1 mixture of Dulbecco's Modified Eagle Medium (DMEM) low glucose and Medium199, containing 10% fetal bovine serum. The following day, non-adherent cells were removed and the medium was replaced with a complete serum-free media modified from [25], that contains: DMEM/F12, 25 mM HEPES, 1.7 μ M insulin, 1 μ M transferrin, 10 nM natrium-selenite, 1 nM tri-iodo-thyronine, 0.2% BSA, 190 nM dexamethasone, 1 mg/l arachidonic acid, 0.5 mg/ml docosahexanoic acid, 100 u/ml penicillin/streptomycin.

Immunofluorescence staining: Cardiomyocyte cultures were grown on an 8-well glass chamber slide (Nalge Nunc International) and prepared for immunofluorescence by washing with phosphate-buffered saline (PBS) followed by fixation with Cytifix buffer (BD Biosciences Pharmingen) for 20 min at room temperature. Cells were then permeabilized either with 0.2% Triton-X 100 or 0.5% saponin for 4 min at room temperature. Non-specific binding sites were blocked by incubation with 1% BSA for 30 min at room temperature and a monoclonal anti-desmin antibody (Sigma) was applied for 1 hr for localization of desmin at the periphery of z-discs. Nuclei were visualized by staining with 4',6'-diamidino-2-phenylindole hydrochloride (DAPI) for 5 min. Slides were mounted with Prolong Antifade Kit (Molecular Probes) and analysed with Nikon Optiphot/2 fluorescence microscope.

Optical Magnetic Twisting Cytometry: The frequency dependence of the mechanical properties of a cardiomyocyte was assessed using optical magnetic twisting cytometry (OMTC) [11, 26]. The OMTC device is an active micro-rheometer where the living cell is sheared between the Petri dish on which the cell is adhering and a microbead. Ferrimagnetic microbead, 4.5 μm in diameter, were coated with a peptide containing the sequence RGD, and added to an individual well for 20 min. Such a microbead attached firmly to the cytoskeleton of the living cell, mainly through membrane integrins. The individual well was then placed on the stage of a microscope equipped with a set of magnetizing and twisting coils. After magnetization of the microbeads, a twisting magnetic field at frequency, f , applied by the twisting coils induced a torque on each microbead, and the resulting displacements of approximately a hundred of microbeads were recorded simultaneously. At a given frequency, the complex modulus $g^*(f)$ is inferred from the ratio of the Fourier transform of the mechanical torque per microbead volume, $\tilde{T}(f)$, to the Fourier transform of the resulting microbead displacement, $\tilde{d}(f)$, and $g^*(f) = \tilde{T}(f)/\tilde{d}(f) = g'(f) + jg''(f)$, with $g'(f)$ the elastic modulus, $g''(f)$ the loss modulus, and $j^2 = -1$. A characteristic of cardiomyocytes in culture is that they spontaneously contract. Before measurements of the complex modulus, spontaneous contractions were stopped by mean of a calcium free media. Measurements were performed over four decades in frequency, from 0.1 Hz to 1 kHz; such a frequency scan was carry out in about 5 min.

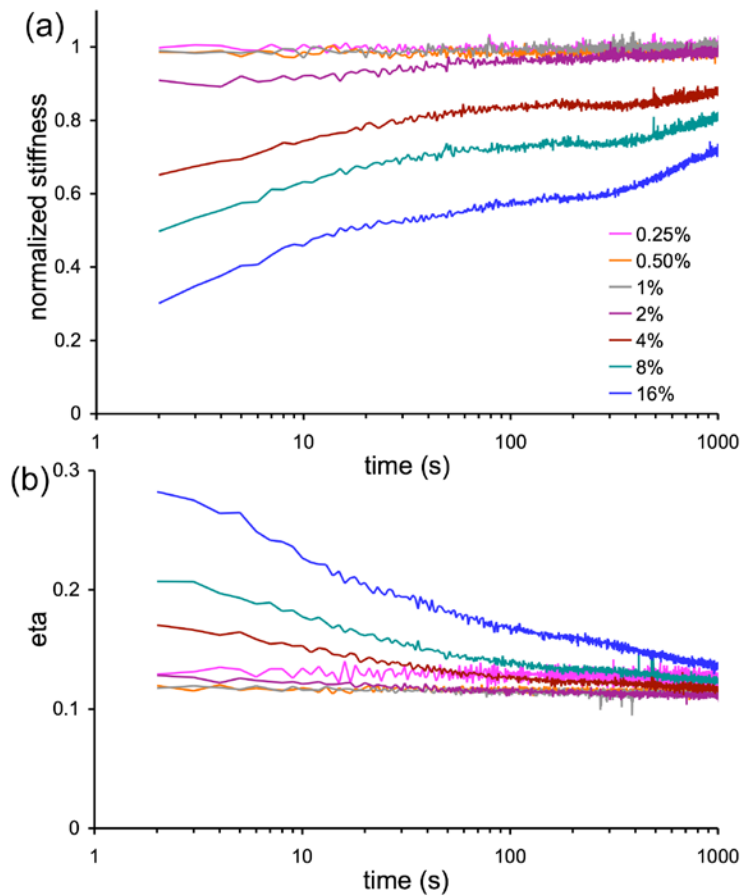
Supplementary Figure 2

Frequency and strain dependence on the elastic modulus, E' , the loss modulus, E'' , and the loss tangent, η . (a) Frequency dependence. After 5 min of maximum isometric contraction using 2×10^{-5} M Ach (system 2), length oscillations of small amplitude (0.5% of L_{ref}) are imposed at frequencies ranging from 10^{-2} Hz to 10^2 Hz. The elastic modulus, E' , of the ASM strip is well described by a weak power law over four decades in frequency, with a power law exponent of about 0.05 (mean \pm standard errors over 7 muscle strips). (b) Strain dependence. After 1 hr of contraction at maximum force using 10^{-4} M Ach (system 1), the amplitude of the imposed length oscillation is increased from 0.25% to 16% of L_{ref} ; the frequency is set at 1 Hz. For small strains, the linear regime is observed; for large strains, E' and E'' progressive decrease (mean \pm standard errors over 4 muscle strips).



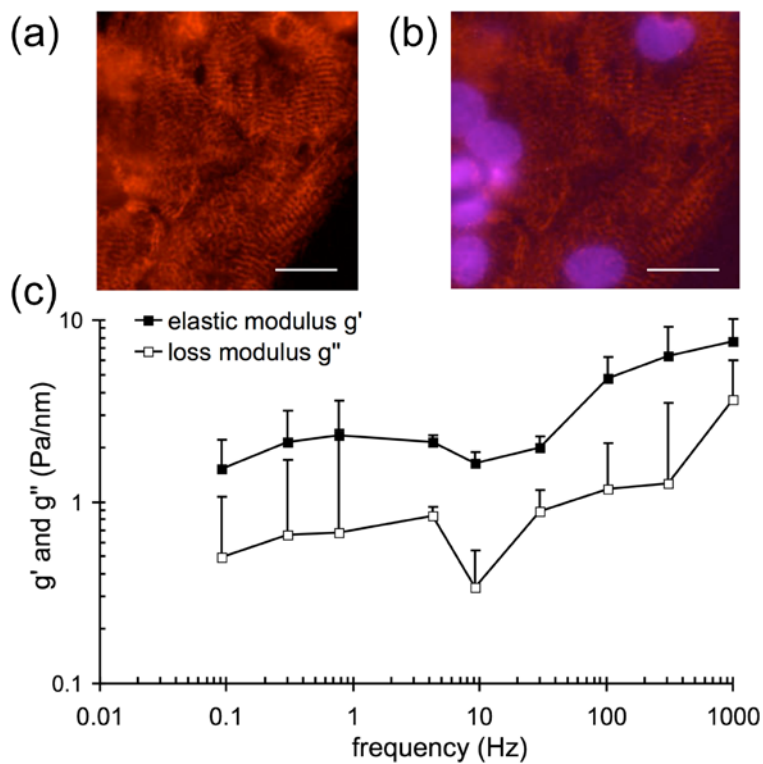
Supplementary Figure 3

Response to a transient stretch. Using system 1, E' and E'' are measured before, during, and after the transient stretch. (a) E' normalized to its value before stretch, for transient stretches ranging from 0.25% to 16% of L_{ref} . In response to a transient shear less than 1%, E' remained mostly unchanged. But as the amplitude of the transient shear is increased, E' becomes progressively more and more depressed. After the prompt drop in stiffness, E' slowly recovers (mean over 4 muscle strips). (b) After stretch, the loss tangent, η , promptly increases in a dose dependent manner, and then slowly recovers (mean over 4 muscle strips). The transient stretch fluidize the ASM strip.



Supplementary Figure 4

Cardiomyocyte measurements (a) A monoclonal anti-desmin antibody was used for immunocytochemical localization of desmin at the periphery of z-discs (red). Z-disc alignments reveal the organization of sarcomeres into myofibrils. Scale bar is 20 μm . (b) Nuclei were visualized by staining with DAPI, showing that myofibrils span several cell lengths. Scale bar is 20 μm . (c) Elastic g' and loss g'' moduli of cardiomyocytes measured using OMTC (median \pm standard error over 752 beads on a similar number of cardiomyocytes). A clear departure from a power law behavior is observed, showing that cytoskeletal dynamics of the cardiomyocyte is not scale-free. This peculiar behavior between 10 and 100 Hz has been observed in striated muscle strip, and is known to correspond to rate constant in the actomyosin ATPase cycle [24].



Supplementary References

- [1] J. J. Fredberg *et al.*, J. Appl. Physiol. **81**, 2703 (1996).
- [2] J. Latourelle, B. Fabry, and J. J. Fredberg, J Appl Physiol **92**, 771 (2002).
- [3] J. J. Fredberg *et al.*, Am J Respir Crit Care Med **156**, 1752 (1997).
- [4] J. J. Fredberg, and D. Stamenovic, J Appl Physiol **67**, 2408 (1989).
- [5] C. M. Hai, and R. A. Murphy, Am J Physiol **254**, C99 (1988).
- [6] C. M. Hai, and R. A. Murphy, Am J Physiol **255**, C86 (1988).
- [7] A. F. Huxley, Prog Biophys Biophys Chem **7**, 255 (1957).
- [8] S. M. Mijailovich, J. P. Butler, and J. J. Fredberg, Biophys J **79**, 2667 (2000).
- [9] H. M. Wyss *et al.*, Phys Rev Lett **98**, 238303 (2007).
- [10] B. Fabry *et al.*, Phys. Rev. Lett. **87**, 148102 (2001).
- [11] B. Fabry *et al.*, Phys. Rev. E. **68**, 041914 (2003).
- [12] G. Lenormand *et al.*, J R Soc Interface **1**, 91 (2004).
- [13] J. Alcaraz *et al.*, Biophys. J. **84**, 2071 (2003).
- [14] N. Desprat *et al.*, Biophys. J. **88**, 2224 (2005).
- [15] M. Balland, A. Richert, and F. Gallet, Eur. Biophys. J. **34**, 255 (2005).
- [16] T. G. Mason, and D. A. Weitz, Physical Review Letters **75**, 2770 (1995).
- [17] T. G. Mason, and D. A. Weitz, Phys. Rev. Lett. **74**, 1250 (1995).
- [18] P. Sollich, Phys. Rev. E. **58**, 738 (1998).
- [19] P. M. Chaikin, and T. C. Lubensky, *Principles of Condensed Matter Physics* (Cambridge University Press, 2000).
- [20] P. Bursac *et al.*, Nat. Mater. **4**, 557 (2005).
- [21] G. Lenormand *et al.*, Phys. Rev. E. **76**, 041901 (2007).
- [22] X. Trepate *et al.*, Nature **447**, 592 (2007).
- [23] R. Krishnan *et al.*, PLoS One **4**, e5486 (2009).
- [24] M. Kawai, and P. W. Brandt, J. Muscle Res. Cell Motil. **1**, 279 (1980).
- [25] P. P. Shields, J. E. Dixon, and C. C. Glembotski, Journal of Biological Chemistry **263**, 12619 (1988).
- [26] B. Fabry *et al.*, J Appl Physiol **91**, 986 (2001).